J|A|C|S
ARTICLES
Published on Web 08/15/2002

Rapid Excited-State Structural Reorganization Captured by Pulsed X-rays

Lin X. Chen,*,† Guy Jennings,‡ Tao Liu,† David J. Gosztola,† Jan P. Hessler,† Donald V. Scaltrito,§ and Gerald J. Meyer§

Contribution from the Chemistry Division and Materials Science Division, Argonne National Laboratory, Argonne, Illinois 60439, and Department of Chemistry, The Johns Hopkins University, Baltimore, Maryland 21210

Received October 2, 2001

Abstract: Visible light excitation of $[Cu^{I}(dmp)_2](BArF)$, where dmp is 2,9-dimethyl-1,10-phenanthroline and BArF is tetrakis(3,5-bis(trifluoromethylphenyl))borate, in toluene produces a photoluminescent, metal-to-ligand charge-transfer (MLCT) excited state with a lifetime of 98 ± 5 ns. Probing this state within 14 ns after photoexcitation with pulsed X-rays establishes that a Cu^{II} center, borne in a Cu^{I} geometry, binds an additional ligand to form a five-coordinate complex with increased bond lengths and a coordination geometry of distorted trigonal bipyramid. The average Cu−N bond length increases in the excited state by 0.07 Å. The transiently formed five-coordinate MLCT state is photoluminescent under the condition studied, indicating that the absorptive and emissive states have distinct geometries. The data represent the first X-ray characterization of a molecular excited state in fluid solution on a nanosecond time scale.

Introduction

Molecular excited states have important applications as luminescent probes and in solar energy conversion, photography, sensing, and displays.[1] A wide variety of theoretical and experimental techniques have been employed to provide insights into the fascinating structures of excited states and the distortions that accompany excited-state relaxation.[2,3] Despite their importance, however, identification of the absolute molecular structure of excited states using X-rays remains elusive. X-ray spectroscopic techniques (including X-ray absorption fine structure, XAFS, and X-ray absorption near edge structure, XANES),[4] which have been tremendously valuable for structural characterization of ground and long-lived transient states,[5−10] have not been successfully applied to excited states. The main obstacle for excited-state structure determination is the lack of pulsed X-ray sources that provide sufficient photons. This obstacle has been circumvented with new generation synchrotron sources that offer X-ray pulses with about 100 ps pulse duration and up to 10^4 times more photons than previous sources.[11] In addition, notable advances in the production of ultrashort, intense X-ray pulses have recently appeared in the literature.[12−17] Here we exploit these advances and report structural studies of

* To whom correspondence and requests for materials should be addressed. E-mail: lchen@anl.gov.
† Chemistry Division, Argonne National Laboratory.
‡ Materials Science Division, Argonne National Laboratory.
§ Department of Chemistry, The Johns Hopkins University.

(1) (a) *Biophysics and Physiobiology of Excitable Membranes*; Adelman, W. J., Ed.; Van Nostrand Reinhold Co.: New York, 1971. (b) *Time-Resolved Fluorescence Spectroscopy in Biochemistry and Biology*; Cundall, R. B., Dale, R. E., Eds.; Plenum Press: New York, 1980. (c) Guillet, J. *Polymer Photophysics and Photochemistry*; Cambridge University Press: Cambridge, 1985. (d) *Fluorescent Chemosensors for Ion and Molecular Recognition*; Czarnick, A. W., Ed.; ACS Symposium Series 538; American Chemical Society: Washington, DC, 1993. (e) Roundhill, D. M. *Photochemistry and Photophysics of Metal Complexes*; Plenum Press: New York, 1994. (f) *Inorganic and Organic Electroluminescence*; Mauch, R. H., Gumlich, H.-E., Eds.; Wissenschaft und Technik Verlag: Berlin, 1996.
(2) (a) Calvert, J. G.; Pitts, J. N. *Photochemistry*; John Wiley & Sons: New York, 1966. (b) Parker, C. A. *Photoluminescence of Solutions*; Elsevier Publishing Co.: New York, 1968. (c) Turro, N. J. *Modern Molecular Photochemistry*; Benjamin Cummings Publishing Co.: Menlo Park, CA, 1978. (d) Lakowicz, J. R. *Principles of Fluorescence Spectroscopy*, 2nd ed.; Kluwer Academic/Plenum Publishers: New York, 1999.
(3) (a) Kasha, M. *Discuss. Faraday Soc.* **1950**, *9*, 14. (b) Strickler, S. J.; Berg, R. A. *J. Chem. Phys.* **1962**, *37*, 814. (c) Freed, K. F.; Jortner, J. *J. Chem. Phys.* **1970**, *52*, 6272. (d) Jortner, J.; Mukamel, S. Preparation and Decay of Molecular Excited States. In *The World of Quantum Chemistry*; Daudei, D., Pullman, B., Eds.; D. Reidel Publishing Co.: Dordrecht, Holland, 1974; pp 145−209.
(4) (a) Sayers, D. E.; Stern, E. A.; Lytle, F. W. *Phys. Rev. Lett.* **1971**, *27*, 1204. (b) Rehr, J. J.; Mustre de Leon, J.; Zabinsky, S. I.; Alberts, R. C. *J. Am. Chem. Soc.* **1991**, *113*, 5135.
(5) Chance, B.; Fischetti, R.; Powers, L. *Biochemistry* **1983**, *22*, 3820.
(6) Mills, D. M.; Lewis, A.; Harootunian, A.; Huang, J.; Smith, B. *Science* **1984**, *223*, 811.
(7) Thiel, D. J.; Livins, P.; Stern, E. A.; Lewis, A. *Nature* **1993**, *362*, 40.
(8) Chen, L. X.; Wang, Z.; Burdett, J. K.; Montano, P. A.; Norris, J. R. *J. Phys. Chem.* **1995**, *99*, 7958.
(9) Chen, L. X.; Bowman, M. K.; Wang, Z.; Montano, P. A.; Norris, J. R. *J. Phys. Chem.* **1994**, *98*, 9457.
(10) Chen, L. X.; Lee, P. L.; Gosztola, D. J.; Svec, W. A.; Montano, P. A.; Wasielewski, M. R. *J. Phys. Chem. B* **1999**, *103*, 3270.
(11) (a) Shenoy, G. K.; Viccaro, P. J.; Mills, D. M. Characteristics of the 7-GeV Advanced Photon Source, Argonne National Laboratory. Report ANL-88-9; Argonne National Laboratory: Argonne, IL, 1988. (b) Knapp, G. S.; Beno, M. A.; You, H. *Annu. Rev. Mater. Sci.* **1996,** *26*, 693.
(12) Schoenlein, R. W.; Chattopadhyay, S.; Chong, H. H. W.; Glover, T. E.; Heimann, P. A.; Shank, C. V.; Zholents, A. A.; Zolotorev, M. S. *Science* **2000**, *287*, 2237.
(13) Rischel, C.; Rousse, A.; Uschmann, I.; Albouy, P. A.; Geindre, J. P.; Audebert, P.; Gauthier, J. C.; Forster, E.; Martin, J. L.; Antonetti, A. *Nature* **1997**, *390*, 490.
(14) Bressler, C.; Chergui, M.; Pattison, P.; Wulff, M.; Filipponi, A.; Abela, R. *Proc. SPIE-Int. Soc. Opt. Eng.* **1998**, *3451*, 108.
(15) Perman, B.; Srajer, V.; Ren, Z.; Teng, T.-Y.; Pradervand, C.; Ursby, T.; Bourgeois, D.; Schotte, F.; Wulff, M.; Kort, R.; Hellingwerf, K.; Moffat, K. *Science* **1998**, *279*, 1946.
(16) Rose-Petruck, C.; Jimenez, R.; Guo, T.; Cavalleri, A.; Siders, C. W.; Raksi, F.; Squier, J. A.; Walker, B. C.; Wilson, K. R.; Barty, C. P. J. *Nature* **1999**, *398*, 310.
(17) Tomov, I. V.; Oulianov, D. A.; Chen, P.; Rentzenpis, P. M. *J. Phys. Chem. B* **1999**, *103*, 7081.

molecular excited states by nanosecond pump−probe XAFS in fluid solution.

This important achievement was made possible with the aid of X-ray pulses from a new generation synchrotron source with a significantly higher X-ray photon flux than was previously available.[11,18,19] A simplified time sequence of the experiment is shown in Figure 1. A laser pulse excites the sample, and a sextuplet X-ray pulse cluster probes the structure of the excited state at its optimal concentration. The goal of this approach is to take a "snapshot" of the thermally equilibrated excited-state structure rather than to follow excited-state relaxation dynamics.

The metal-to-ligand charge-transfer (MLCT) excited states of cuprous diimine compounds were chosen in part because of the compelling evidence described in the literature for novel structural reorganization following light absorption.[20] These reorganization processes are relevant to "gated" electron transfer in proteins[21] and model systems[22] as well as in new classes of molecular devices[23] and solar energy conversion materials.[24] Therefore, these studies not only represent a proof-of-concept example of excited-state characterization but also provide new insights into the dynamics for structural reorganization important in biology and chemistry.

The origin of the photodriven structural change can be understood by considering light absorption by a cuprous diimine compound, such as $Cu^I(dmp)_2^+$, where dmp is 2,9-dimethyl-1,10-phenanthroline, eq 1.

$$Cu^I(dmp)_2^+ + h\nu \rightarrow Cu^{II}(dmp^-)(dmp)^{+}* \qquad (1)$$

The Cu(I) ground state has a d^{10} electronic configuration with pseudo-tetrahedral geometry.[25] Absorption of a visible photon promotes an electron from copper to a dmp ligand, formally generating a MLCT excited state with a Cu(II) center coordinated to one reduced and one neutral dmp ligand. The Cu(II) center in the excited state has a d^9 electron configuration and is subject to a Jahn−Teller distortion.[26] The observations of large "Stokes-like" shifts between the absorption and photoluminescence and "exciplex" quenching represent strong evidence that the excited state adopts a more Cu(II)-like geometry.[20,25] The Jahn−Teller distortion is also clearly manifest in the crystal structures of Cu(II) bipyridine and phenanthroline compounds that reveal distorted square pyramidal or trigonal-bipyramidal geometries with an additional ligand derived from a solvent molecule or counterion.[25,26]

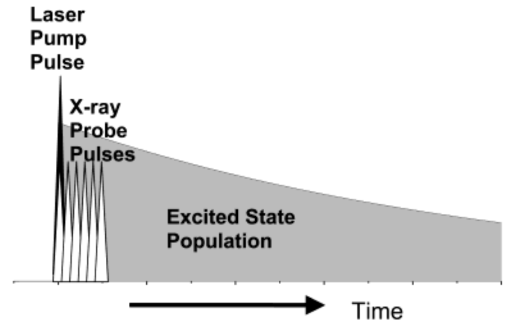

Figure 1. Experimental time sequence used in this work. The laser pump pulse (black triangle) was overlapped with the first X-ray pulse of a sextuplet cluster (white triangles). This time sequence allowed a "snapshot" of the thermally equilibrated excited-state structure to be taken when its population was optimal.

Therefore, for this specific study, light absorption by Cu(I) diimine compounds instantaneously creates a Franck−Condon state with a Cu(II) excited state in a Cu(I) geometry. Within our instrument response time, this state rapidly undergoes vibrational relaxation and Jahn−Teller distortions to yield an emissive, thermally equilibrated excited state that lives for about 100 ns, $\tau = 98 \pm 5$ ns. The purpose of the study is to capture the structure of this MLCT state at its optimal concentration. In particular, this work investigates whether the MLCT transition is a whole or partial charge transfer from Cu(I) to the ligand, and how the resulting thermally equilibrated MLCT-state structure differs from the corresponding Cu(I) and Cu(II) compounds in the ground state.

Experimental Section

Synthesis. The $[Cu^I(dmp)_2](PF_6)$ and $Cu^I(dmp)_2(NO_3)$ were synthesized according to previously published procedures.[27−30] The $[Cu^I(dmp)_2](BArF)$ was synthesized via the metathesis of $[Cu^I(dmp)_2](PF_6)$ with sodium tetrakis(3,5-bis(trifluoromethylphenyl))borate (Boulder Scientific) in a 1:1 ratio in toluene. The $[Cu^{II}(dmp)_2(NO_3)](NO_3)$ was synthesized following a previously published protocol.[31]

(18) Chen, L. X.; Jäger, W. J. H.; Jennings, G.; Gosztola, D. J.; Munkholm, A.; Hessler, J. P. *Science* **2001**, *292*, 262.
(19) (a) Chen, L. X. *J. Elect. Spectrosc., Relat. Phenom.* **2001**, *119*, 161. (b) Jennings, G.; Jäger, W. J. H.; Chen, L. X. *Rev. Sci. Instrum.* **2002**, *72*, 362.
(20) (a) Kalyanasundaram, K. *Photochemistry of Polypyridine and Porphyrin Complexes*; Academic Press: London, 1992; Chapter 9. (b) Scaltrito, D. V.; Thompson, D. W.; O'Callaghan, J. A.; Meyer, G. J. *Coord. Chem. Rev.* **2000**, *208*, 243. (c) Armaroli, N. *Chem. Soc. Rev.* **2001**, *30*, 113.
(21) (a) Lumry, R.; Eyring, H. *J. Phys. Chem.* **1954**, *58*, 110−120. (b) Vallee, B. L.; Williams, R. J. P. *Proc. Natl. Acad. Sci. U.S.A.* **1968**, *59*, 498−505. (c) Holm, R. H.; Kennepohl, P.; Solomon, E. I. *Chem. Rev.* **1996**, *96*, 2239.
(22) (a) Meagher, N. E.; Juntunen, K. L.; Salhi, C. A.; Ochrymowycz, L. A.; Rorabacher, D. B. *J. Am. Chem. Soc.* **1992**, *114*, 10411−10420. (b) Flanagan, S.; Dong, J.; Haller, K.; Wang, S.; Scheidt, W. R.; Scott, R. A.; Webb, T. R.; Stanbury, D. M.; Wilson, L. J. *J. Am. Chem. Soc.* **1997**, *119*, 8857−8864.
(23) Collin, J. P.; Dietrich-Buchecker, C.; Gavina, P.; Jimenez-Molero, M. C.; Sauvage, J.-P. *Acc. Chem. Res.* **2001**, *34*, 477.
(24) (a) Breddels, P. A.; Blassie, G.; Casdonte, D. J.; McMillin, D. R. *Ber. Bunsen-Ges. Phys. Chem.* **1984**, *88*, 2. (b) Alonso-Vante, N.; Nierengarten, J. F.; Sauvage, J. P. *J. Chem. Soc., Dalton Trans.* **1994**, 1649. (c) Ruthkosky, M.; Kelly, C. A.; Castellano, F. N.; Meyer, G. J. *J. Am. Chem. Soc.* **1997**, *119*, 12004.
(25) (a) Stephens, F. S. *J. Chem. Soc., Dalton Trans.* **1972**, 1350. (b) Stephens, F. S.; Tucker, P. A. *J. Chem. Soc., Dalton Trans.* **1973**, 2293. (c) Kaiser, J.; Brauer, G.; Schroder, F. A.; Taylor, I. F.; Rasmussen, S. E. *J. Chem. Soc., Dalton Trans.* **1974**, 1490. (d) Anderson, O. P. *Inorg. Chem.* **1975**, *14*, 730. (e) Harrison, W. D.; Hathaway, B. J.; Kennedy, D. *Acta Crystallogr., Sect. B* **1979**, *35*, 2301. (f) Harrison, W. D.; Hathaway, B. J. *Acta Crystallogr., Sect. B* **1979**, *35*, 2910. (g) Harrison, W. D.; Kennedy, D. M.; Power, M.; Sheahan, R.; Hathaway, B. J. *J. Chem. Soc., Dalton Trans.* **1981**, 1556. (h) Tran, D.; Skelton, B. W.; White, A. H.; Laverman, L. E.; Ford, P. C. *Inorg. Chem.* **1998**, *37*, 2505.
(26) Coordination numbers greater than five are known for nonluminescent copper bis-phenanthroline compounds with unsubstituted 1,10-phenathroline ligands. They are not known for luminescent complexes where substituents in the 2- and 9- positions are required.
(27) (a) Blaskie, M. W.; McMillin, D. R. *Inorg. Chem.* **1980**, *19*, 3519. (b) McMillin, D. R.; Kirchhoff, J. R.; Goodwin, K. V. *Coord. Chem. Rev.* **1985**, *64*, 83.
(28) (a) Cunningham, C. T.; Cunningham, K. L. H.; Michalec, J. F.; McMillin, D. R. *Inorg. Chem.* **1999**, *38*, 4388. (b) Cunningham, C. T.; Moore, J. J.; Cunningham, K. L. H.; Fanwick, P. E.; McMillin, D. R. *Inorg. Chem.* **2000**, *39*, 3638.
(29) Miller, M. T.; Ganzel, P. K.; Karpisihin, T. B. *J. Am. Chem. Soc.* **1999**, *121*, 4292.
(30) Felder, D.; Nierengarten, J. F.; Barigelletti, F.; Ventura, B.; Armaroli, N. *J. Am. Chem. Soc.* **2001**, *123*, 6291.
(31) Riesgo, E. C.; Hu, Y.-Z.; Bouvier, F.; Thummel, R. P.; Scaltrito, D. V.; Meyer, G. J. *Inorg. Chem.* **2001**, *40*, 3413.
(32) Antonio, M. R.; Soderholm, L.; Song, I. J. *Appl. Electrochem.* **1997**, *27*, 784.
(33) (a) Hamalainen, R.; Algren, M.; Turpeinen, U.; Raikas, T. *Cryst. Struct. Commun.* **1979**, *8*, 75. (b) Van Meerssche, M.; Germain, G.; Declercq, J. P. *Cryst. Struct. Commun.* **1981**, *10*, 47.

Electrolysis for in Situ XAFS. Bulk electrolysis of 2 mM $Cu^{I}(dmp)_2^+$ in 0.1 M Bu_4NPF_6 acetonitrile was carried out using a microprocessor-controlled potentiostat (Princeton Applied Research, model 273) and a standard three-electrode arrangement in a previously described spectroelectrochemical cell designed for XAFS use.[32] The working electrode was a 3 cm^2 platinum mesh, and the auxiliary electrode was a platinum wire located in a portion of the cell separated by a porous glass frit. The applied potential was measured versus an aqueous Ag^+/AgCl reference electrode. Prior to oxidation, the solution was purged with acetonitrile-saturated nitrogen gas. The nitrogen gas continued to bubble through the solution during electrolysis to aid in stirring the solution. After approximately 20 min at +0.80 V, the complex was completely oxidized. During the remainder of the experiments, the solution was blanketed with a stream of nitrogen gas.

Pump−Probe XAFS. The copper K-edge (8.979 keV) XANES and XAFS measurements were conducted at a wiggler beamline, 11ID-D, Basic Energy Science Synchrotron Research Center of the Advanced Photon Source at Argonne National Laboratory. The details of the experimental setup were described elsewhere.[18,19] Briefly, the pump laser pulses were from the second harmonic output of a Nd−YLF laser (λ = 527 nm, 1 kHz repetition rate, 1 mJ/pulse, and 5 ps fwhm), and the probe X-ray pulses (a sextuplet X-ray cluster of 14.2 ns, 271 kHz repetition rate) were from the synchrotron running with an asymmetric timing mode where a sextuplet X-ray pulse cluster was separated in time from other pulses in the storage ring.[18,19] The time delay between the pump and the probe was adjusted so that the laser pulse overlapped with the first X-ray pulse in the sextuplet pulse cluster (Figure 1). The laser pump and X-ray probe beams were intersected at a continuously flowing sample stream of 2 mM $[Cu^{I}(dmp)_2]$(BArF) toluene solution. The thickness of the sample stream was about 0.5 mm. A Ge detector array was used to detect the X-ray fluorescence of the sample. The different repetition rates of the laser pump and X-ray probe pulses required timing the data acquisition to isolate those signals that correspond to the sample being simultaneously illuminated with a laser and X-ray pulses.[18,19] Therefore, the Ge detector array signals were split into two equal parts connected separately to two scaler modules. The first module processed only X-ray signals from the sextuplet X-ray probe pulse cluster that coincided with the laser pump pulse, and the second module processed signals from all X-ray pulses. The output from the former was used to obtain XANES and XAFS spectra of the laser-illuminated sample, and that of the latter, the spectra of the ground state. Therefore, the pump−probe cycles were repeated at a laser pulse repetition rate of 1 kHz until the XAFS spectrum of the laser-excited sample had a satisfactory signal-to-noise ratio to establish the oxidation state, the coordination geometry, and the local fine structure around the metal center. The total data acquisition time was approximately 20 h.

A nanosecond transient UV−vis absorption apparatus with the same laser and similar sample conditions was performed prior to X-ray experiments to ensure that the MLCT excited state was generated with the efficiency expected. The sample integrity was also monitored periodically by UV−vis spectroscopy during the pump−probe XAFS experiment and was changed every 3−4 h to ensure sample integrity.

Data Analysis of XANES and XAFS Spectra. The measured XANES spectrum of the laser-illuminated sample contains contributions from the ground and the MLCT excited states. The XANES spectrum of the MLCT state alone was calculated by subtracting the appropriate fraction of ground-state spectrum from the measured spectrum. The fraction of the ground state that remained in the laser-illuminated sample was determined by the Beer−Lambert law and the measured irradiance, sample concentration, and extinction coefficient with an assumed intersystem crossing yield of unity.

For XAFS data analysis, $Cu^{I}(dmp)_2(NO_3)$[33] and $Cu^{II}(dmp)_2(NO_3)_2$[33] solids were used as references for the phase and amplitude of the ground state and the MLCT state. The coordination number of four and an average Cu−N distance of 2.07 Å were used for $Cu^{I}(dmp)_2(NO_3)$, in accordance with its crystal structure.[33] Similarly, the coordination number of five (four N atoms and one O atom) and the average nearest-neighbor distance of 2.09 Å were used for $Cu^{II}(dmp)_2(NO_3)_2$.[33] WinXAS 97[34] was used for data analysis following standard procedures.[35] The experimentally collected data were fit to the equation

$$\chi(k) = \sum F_i(k) S_0^{\,2}(k) N_i/(kR_i^{\,2}) \exp(-2\sigma_i^{\,2}k^2) \sin[2kR_i + \phi_i(k)]$$

where $F(k)$ is the magnitude of the backscattering, S_0 the amplitude reduction factor, N the coordination number, R the average distance, σ^2 the Debye−Waller factor, and ϕ_i the phase shift; the subscript indicates the ith atom, and k is the electron wavevector.

Photoluminescence. Corrected photoluminescence (PL) spectra were obtained with a Spex Fluorolog that had been calibrated with a standard tungsten−halogen lamp using procedures given by the manufacturer. Quantum yields were measured by the optically dilute technique with $Ru(bpy)_3^{2+}$ as a standard.[36] Time-resolved PL measurements were made as previously described.[37]

UV−Vis Absorption. Ground-state absorption spectra were acquired at ambient temperature in air using a Hewlett-Packard 8453 diode array spectrometer. Nanosecond time-resolved absorption measurements were made with an apparatus that has been previously described.[38]

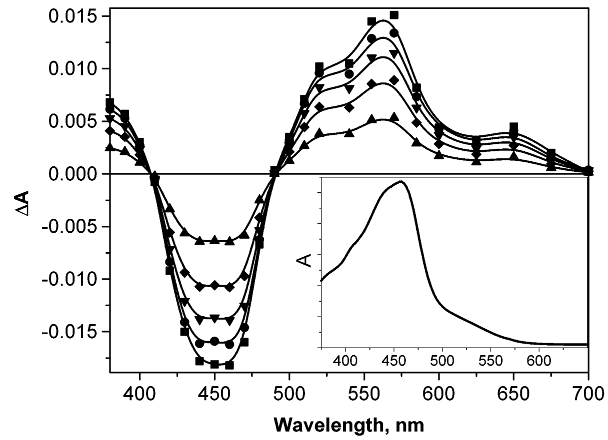

Figure 2. Absorption difference spectra obtained after pulsed 532 nm light excitation (5−8 mJ/cm^2, 8 ns fwhm) of $[Cu^{I}(dmp)_2]$(BArF) in argon-saturated toluene at room temperature. The spectra are shown at the following delay times: 0 (■), 10 (●), 25 (▼), 50 (◆), and 100 ns (▲). The inset displays the ground-state absorption spectrum of $[Cu^{I}(dmp)_2]$(BArF) in toluene at room temperature.

Results

The absorption spectrum of $[Cu^{I}(dmp)_2]$(BArF) in toluene displayed characteristic broad MLCT bands in the visible region centered at 460 nm (Figure 2, inset). Light excitation into these bands resulted in room-temperature photoluminescence with a corrected maximum at 710 nm, an emission quantum yield ϕ_{em} = 1.12 × 10^{-3}, and a lifetime of 98 ns. Assuming an intersystem crossing yield of unity, a radiative rate constant, k_r, of 1.14 × 10^4 s^{-1} and a nonradiative rate constant, k_{nr}, of 1.02 × 10^7 s^{-1} were calculated. Time-resolved absorption spectroscopy yielded difference spectra with positive absorption bands centered at ~350 and ~580 nm that were characteristics of the reduced dmp ligand and a bleach of the ground-state absorption at

(34) Ressler, T. *J. Synch. Radiat.* **1998**, *5*, 118.
(35) Stern, E. A.; Sayers, D. E.; Lytle, F. W. *Phys. Rev. B* **1975**, *11*, 4836.
(36) Demas, J. N.; Crosby, G. A. *J. Phys. Chem.* **1971**, *75*, 991.
(37) Castellano, F. N.; Heimer, T. A.; Thandasetti, M.; Meyer, G. J. *Chem. Mater.* **1994**, *6*, 1041.
(38) Kelly, C. A.; Thompson, D. W.; Farzad, F.; Stipkala, J. M.; Meyer, G. J. *Langmuir* **1999**, *15*, 7047.

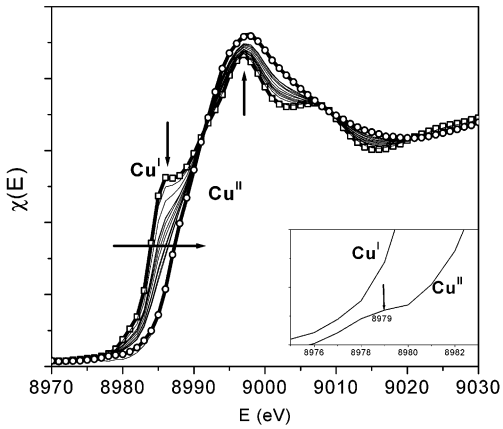

Figure 3. In situ XANES spectra of $[Cu^I(dmp)_2](BArF)$ in acetonitrile at room temperature during the electrolysis at 0.8 V versus an aqueous Ag^+/AgCl electrode, where Cu^I was oxidized to Cu^{II}. E is the photon energy of the X-ray, and $\mu(E)$ is proportional to the amount of X-ray absorbed by the sample. The initial spectrum of $Cu^I(dmp)_2^+$, before the electrolysis, is shown as open squares, and the final spectrum of the Cu(II) product is shown as open circles. Eight intermediate spectra are also shown. The arrows indicate the directions of the changes in the spectra during the electrolysis. The inset shows the pre-edge region of the starting and ending spectra only.

460 nm (Figure 2). Clean isosbestic points and first-order kinetics were observed with lifetimes that agree, within experimental error, with those measured independently by time-resolved photoluminescence spectroscopy. Steady-state UV−vis absorption data collected before and after these transient studies revealed no experimental evidence for sample decomposition.

To identify the oxidation state of copper in the MLCT excited state, we first measured copper K-edge XANES spectra of the ground-state $Cu^I(dmp)_2^+$ and the Cu(II) product obtained by in situ electrolysis (Figure 3). The following spectral differences were observed between the Cu^I and Cu^{II} species: (1) a transition edge shift that was 3 eV higher for Cu^{II} than for Cu^I, reflecting the higher positive charges in the former; (2) a shoulder feature at 8985 eV representing a 1s-to-4p_z transition that was pronounced in Cu^I and missing from Cu^{II}, typically observed for transformation from four- to five- or six-coordinate geometry, because the 4p_z orbital was localized in the former, consistent with a localized-to-delocalized transition of the 4p_z orbital;[39] (3) an intensity of the 8997 eV peak that was higher for Cu^{II} than for Cu^I, suggesting a higher coordination number in the former, because of the proportionality of the oscillation amplitude with the coordination number; and (4) a pre-edge feature at 8979 eV (Figure 4 inset) attributed to a 1s → 3d transition that was only present for the Cu^{II} (d^9) compound with one vacancy in 3d orbitals. These XANES spectral features of $Cu^I(dmp)_2^+$ and the Cu(II) oxidation product agree well with previously reported spectra where the $Cu^{II}(dmp)_2^+$ complex in acetonitrile was identified to be pentacoordinated.[40]

XANES spectra of the ground-state and laser-illuminated $Cu^I(dmp)_2^+$ solution are shown in Figure 4A. The laser-illuminated $Cu^I(dmp)_2^+$ solution had a reduced shoulder feature at 8985 eV compared to the ground state and a weak pre-edge feature at

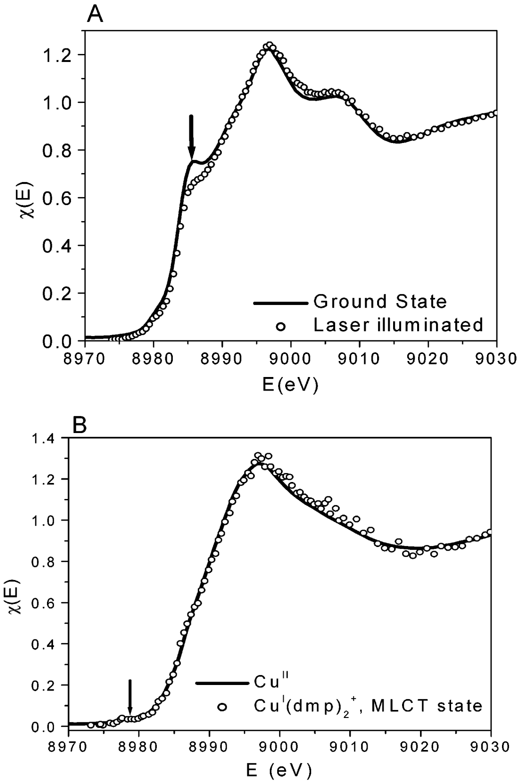

Figure 4. (A) XANES spectra of $[Cu^I(dmp)_2](BArF)$ in toluene with and without laser illumination. (B) XANES spectrum of the MLCT state generated by subtraction of the ground-state contributions to the spectrum of the laser-illuminated sample followed by normalization to 100% MLCT state (see text). The XANES spectrum of the Cu(II) oxidation product from Figure 3 is shown for comparison. $\chi(E)$ is the interference function, defined as $[\mu(E) - \mu^0(E)]/\mu^0(E)]$, where $\mu(E)$ and $\mu^0(E)$ are absorption coefficients of $[Cu^I(dmp)_2](BArF)$ and isolated copper atoms, respectively.

8979 eV. Because such spectral changes were absent when the sample was not illuminated or when the detection was not gated, the spectral changes were due to generation of the MLCT excited state.

The XANES spectrum for the laser-illuminated sample shown in Figure 4A (circles) represents an algebraic sum of both the MLCT excited and ground states in the solution at the time of the X-ray probe. As mentioned in the Experimental Section, the fraction of excited-state molecules was calculated on the basis of the Beer−Lambert law. For the data shown, the laser-illuminated spectrum was comprised of 80% ground state and 20% MLCT excited state. Therefore, subtraction of this fraction of the known $Cu^I(dmp)_2^+$ spectrum from that of the laser-illuminated sample followed by normalization allowed abstraction of the MLCT-state spectrum in Figure 4B (circles).

Bond lengths from the copper to the ligands for the MLCT excited state of $Cu^I(dmp)_2^+$ were also quantified. Figure 5 displayed XAFS and Fourier-transformed XAFS spectra for the ground-state and laser-illuminated $Cu^I(dmp)_2^+$. The magnitude of the Cu−N peak in Figure 5B for the laser-illuminated $Cu^I(dmp)_2^+$ was higher and shifted to a longer distance compared to that in the ground state, suggesting an increase in the coordination number of copper and the lengthening of the average Cu−N bond. The results of data analysis for the nearest-neighbor distances from the copper ion are listed in Table 1. For the ground-state $Cu^I(dmp)_2^+$, an average Cu−N bond

(39) (a) Smith, T. A.; Penner-Hahn, J. E.; Berding, M. A.; Doniach, S.; Hodgson, K. O. *J. Am. Chem. Soc.* **1985**, *107*, 5945. (b) Kau, L.-S.; Spira-Solomon, D. J.; Penner-Hahn, J. E.; Hodgson, K. O.; Solomon, E. I. *J. Am. Chem. Soc.* **1987**, *109*, 6433.
(40) Elder, R. C.; Lunte, C. E.; Rahman, A. F. M. M.; Kirchhoff, J. R.; Dewald, H. D.; Heineman, W. R. *J. Electroanal. Chem.* **1988**, *240*, 361.

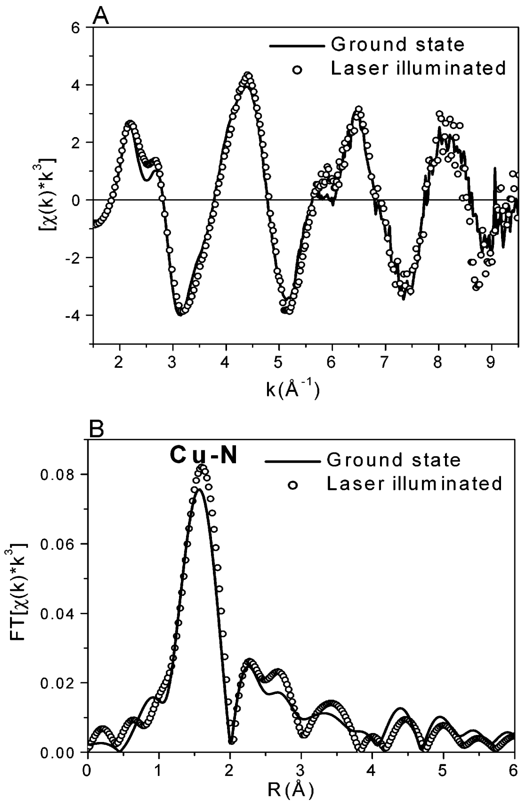

Figure 5. (A) XAFS spectra of the ground-state and laser-illuminated $[Cu^{I}(dmp)_2](BArF)$ in toluene, where the frequency of the oscillation is related to the bond distance from the copper atom and the amplitude of the oscillation is related to the coordination number of the copper as well as the Debye−Waller factor (see equation in the Experimental Section), where k is the X-ray wave vector and $\chi(k)$ is the interference function in k space. (B) Fourier-transformed XAFS spectra of (A), where each peak represents one average distance between the copper atom and its neighbors. R is the distance, in angstroms, from the central copper atom. The peak corresponding to the nearest neighbors is labeled. The shift of the peak and the amplitude change reflect structural changes. The light-illuminated $Cu^{I}(dmp)_2^+$ solution has a longer average Cu−N distance and a higher coordination number than the ground state. The spectra are not corrected with phase factors, so the peaks appear at distances smaller than the real distances. The details of the data analysis are described in the Experimental Section, and the phase-corrected structural parameters can be found in Table 1.

Table 1. Ground- and MLCT-Excited-State Structures[a]

	coordination number	R (Å)[c]	σ^2 (Å^2)[d]
ground-state $Cu^{I}(dmp)_2^{+}$ [b]	4.0 ± 0.5	2.06 ± 0.02	0.0009
with light (fit 1 bond length)[b]	4.5 ± 0.5	2.07 ± 0.02	−0.0008
with light (fit 2 bond lengths)[e]	4.0 ± 0.5 (80%)	2.06 ± 0.02	0.004
	4.0 ± 1.0 (20%)	2.13 ± 0.04	−0.009

[a] Only the nearest neighboring atomic shell is presented. [b] Using $Cu^{I}(dmp)_2NO_3$ solid as reference with an average Cu−N distance of 2.07 Å and a coordination number of four. This one-distance model resulted in a poor fit to the experimental data. [c] Bond distance. [d] Debye−Waller factors. [e] Using $Cu^{I}(dmp)_2NO_3$ and $Cu^{II}(dmp)_2(NO_3)^+$ (average Cu−N distance of 2.09 Å and a coordination number of five) as references for the first and the second distances, respectively.

distance of 2.06 Å and a coordination number of four were obtained. The Cu−N bond distances for the laser-illuminated sample could not be adequately modeled with a single distance, so a two-distance fit was carried out, resulting in a much better fit with two Cu−N bond distances at 2.06 and 2.13 Å with a relative ratio of 80:20. Obviously, the former was from the ground-state molecules and the latter from the MLCT excited-state molecules. Thus, the average Cu−N bond distance in the MLCT state increased by 0.07 Å from that of the ground state. Because the accuracy for coordination number determination from XAFS analysis is normally 10−20%, it is difficult to establish whether the copper coordination number is four or five in the MLCT state from this analysis alone. However, the XANES features of the MLCT state described above and the increase of the Cu−N peak height in Figure 5B support an increase in copper coordination number in the MLCT state.

Discussion

The results presented above have clearly demonstrated X-ray characterization of a molecular excited-state structure under experimentally useful conditions of fluid solution and room temperature. This exciting observation appears to be unprecedented but may be extended to other inorganic and organic molecular excited states. Below we describe the details of the structure determination for the Cu(I) MLCT excited states and the implications of these results on the molecular reorganization novel to Cu(II/I) charge transfer.

X-ray Evidence for the MLCT Excited-State Structure of $Cu^{I}(dmp)_2^+$. The transition edge in a K-edge XANES spectrum is related to the energy required for ejecting a 1s electron to the continuum and is therefore sensitive to the oxidation state of the X-ray absorbing atom. The transition edge position generally shifts to higher energy with increased oxidation state[41] and is also sensitive to the chemical nature of the coordinating ligands. The XANES fine structure corresponds to transitions from the 1s core orbital to valence orbitals that participate in chemical bonding, subject to selection rules. Therefore, XANES spectra are extremely powerful for the elucidation of the coordination environment of transition metal compounds.[39,40−42]

One of the issues we sought to explore was whether light absorption by $Cu^{I}(dmp)_2^+$ resulted in whole or partial charge transfer from Cu(I) to a dmp ligand. The copper K-edge XANES spectra for $Cu^{I}(dmp)_2^+$ and the in situ oxidation product were used for comparisons with the XANES spectrum for the MLCT excited state in Figure 4B. Partial charge transfer was expected to manifest itself in a transition edge position intermediate between the Cu^{I} and Cu^{II} XANES spectra. However, the MLCT and the Cu^{II} had virtually identical edge positions, indicative of complete Cu(I)-to-dmp charge transfer in the MLCT state. Additional evidence for complete charge transfer in the MLCT state comes from the appearance of a pre-edge peak at 8979 eV. This peak is due to the 1s-to-3d transition induced by the X-ray photon, which is feasible only for Cu(II) ($3d^9$) with one vacancy in 3d orbitals, but not for Cu(I) ($3d^{10}$) with no vacancy.

The coordination geometry of copper in the MLCT excited state can also be revealed from the XANES spectra in Figure 4B. The distinctive shoulder feature at 8985 eV in the ground state of $Cu^{I}(dmp)_2^+$ has been attributed to the $1s \rightarrow 4p_z$ transition when the $4p_z$ is localized on the copper with a square-planar or tetrahedral geometry.[39] When the fifth and sixth ligands bind to the metal along the z direction, the $4p_z$ orbital delocalizes and the peak due to the $1s \rightarrow 4p_z$ transition is smeared out,

(41) Koningsberg, D. C., Prins, R., Eds. *X-ray Absorption: Principles, Applications, Techniques of EXAFS, SEXAFE and XANES*; John Wiley & Sons: New York, NY; 1988.
(42) Westre, T. E.; Kennepohl, P.; DeWitt, J. G.; Hedman, B.; Hodgson, K. O.; Solomon, E. I. *J. Am. Chem. Soc.* **1997**, *119*, 6297.

resulting in a smooth transition edge.[39] Such changes in the transition edge due to the ligation have been well documented for metalloporphyrins with and without one or two axial ligands,[18,38] as well as other transition metal complexes.[39,41,42] Therefore, the rather smooth rising edge in the XANES spectrum of the MLCT state in Figure 4B is consistent with a penta- or hexacoordination geometry of the copper center. The steric hindrance from the methyl groups on the phenanthroline ligands inhibits octahedral geometries, so a pentacoordinate MLCT structure is more likely. Since the observed pre-edge feature at 8979 eV due to the quadrupole-allowed 1s → 3d transition[43] is weak yet detectable, the coordination is likely a distorted trigonal-bipyramidal or a distorted square-pyramidal geometry.

The results from the XAFS data analysis listed show an average Cu−N bond expansion by 0.07 Å in the MLCT excited state. Previous excited-state Raman studies are consistent with localization of the excited state on one dmp ligand;[44] however, we are unable to resolve discrete Cu−N distances from the current experimental X-ray data. The observed Cu−N bond elongation in the MLCT state agrees with recent theoretical predictions that addition of a water ligand to a $Cu^I(dmp)_2^+$ excited state should substantially increase the Cu−N bond distance.[45] For comparison, the X-ray crystallographically determined bond lengths indicate that the average Cu−N bond length is 0.02 Å longer for $Cu^{II}(dmp)_2NO_3^{2+}$ than for $Cu^I(dmp)_2^+$.[33] Although the XAFS data fitting procedure does not allow us to unambiguously distinguish the coordination number of the excited state, the XANES evidence presented above and the increased amplitude of the Cu−N peak for the laser-illuminated sample (Figure 5B) strongly support a five-coordinate $Cu^I(dmp)_2^+$ MLCT excited state, despite the uncertainly on the coordination number solely from the XAFS data fitting.

Implications for Copper Diimine Excited States. The coincidence of the $Cu^I(dmp)_2^{+*}$ lifetimes measured by time-resolved absorption and photoluminescence spectroscopies indicates that the same thermally equilibrated MLCT excited state is observed by both techniques and strongly suggests that this is the same state probed by X-ray pulses. The X-ray data provide convincing evidence that there are five nearest neighbors in the copper coordination sphere. In addition, copper in the MLCT excited state is formally a 17-electron d^9 Cu(II) system prone to the addition of a fifth ligand, and there exists a preponderance of indirect literature evidence that indicates a five-coordinate excited state.[20] Below we discuss the relevant literature results and the implications of an emissive five-coordinate thermally equilibrated excited state.

A photodriven increase in the copper coordination number has previously been invoked to explain the quenching of copper excited states by Lewis bases.[46] Extensive studies by McMillin and co-workers have provided compelling evidence that Lewis base addition to copper excited states in dichloromethane forms a five-coordinate excited-state complex, or "exciplex".[46] Copper diimine excited states, and MLCT excited states in general,[47] are known to follow Jortner's energy gap law, wherein the nonradiative rate constant increases exponentially with decreasing ground state−excited state energy separation.[3c,20b] Exciplex quenching can be understood on this basis: coordination of a fifth ligand stabilizes the excited state, thereby decreasing the energy gap and promoting nonradiative decay. With $Cu^I(dmp)_2^{+*}$, the exciplexes that have been identified decrease the energy gap to the extent that nonradiative decay is the sole relaxation pathway and no emission has been detected. Copper diimine compounds with more sterically bulky ligands, on the other hand, inhibit exciplex formation, and room-temperature photoluminescence is often observed, even in Lewis basic solvents.[20b,31,48] For these sterically congested compounds, the absorption spectra are solvent independent, while the photoluminescence spectra red shift and the excited state lifetimes decrease significantly in more coordinating solvents.[31,48] These facts stated in the literature are consistent with emission from a five-coordinate excited state with weak excited state−solvent interactions that stabilize the excited state but not to the extent that nonradiative decay is the sole relaxation pathway. However, we emphasize that photoluminescence is an indirect method for determining changes in coordination number.

Our hypothesis is that $Cu(dmp)_2^{+*}$ in toluene behaves in a manner similar to that reported previously for sterically bulky copper compounds. A weak adduct is formed in the excited state, presumably with toluene or the BArF anion, that stabilizes the excited state but not to the degree where radiative decay is noncompetitive, $k_r = 1.14 \times 10^4\ s^{-1}$ and $k_{nr} = 1.02 \times 10^7\ s^{-1}$. There is no experimental evidence that precludes the existence of a related five-coordinate excited state for $Cu^I(dmp)_2^{+*}$ in dichloromethane, although our attempts to characterize it by X-rays were frustrated by irreversible photochemistry.[49] We anticipate stronger ion-pairing in toluene than in dichloromethane; however, it is difficult to predict which solvent and/or counterion would be more nucleophilic. The higher energy emission maximum and longer lifetime in toluene only suggest weaker excited-state interactions and/or less reorganization for $Cu(dmp)_2^{+*}$ than in dichloromethane.[20c] We emphasize that the evidence for exciplex formation from previous work is compelling but indirect. Exciplexes were just inferred for cases where strong excited-state adducts completely quenched the excited state. This underscores the utility of X-ray techniques that provide a direct method for determination of the excited-state coordination environment.

The conclusion that the excited state is five-coordinate has important implications in copper excited states (Figure 6).[50]

(43) Shulman, R. G.; Yafet, Y.; Eisenberger, P.; Blumberg, W. E. *Proc. Natl. Acad. Sci. U.S.A.* **1976**, *73*, 1384.
(44) Gordon, K. C.; McGarvey, J. J. *Inorg. Chem.* **1991**, *30*, 2986.
(45) Sakaki, S.; Mizutani, H.; Kase, Y. *Inorg. Chem*. **1992**, *31*, 4575.
(46) (a) McMillin, D. R.; Kirchoff, J. R.; Goodwin, K. V. *Coord. Chem. Rev.* **1985**, *64*, 83. (b) Palmer, C. E. A.; McMillin, D. R.; Kirmaier, C.; Holten, D. *Inorg. Chem.* **1987**, *26*, 3167. (c) Crane, D. R.; DiBenedetto, J.; Palmer, C. E. A.; McMillin, D. R.; Ford, P. C. *Inorg. Chem.* **1988**, *27*, 3698. (d) Everly, R. M.; McMillin, D. R. *Photochem. Photobiol.* **1989**, *50*, 711. (e) Stacy, E. M.; McMillin, D. R. *Inorg. Chem.* **1990**, *29*, 393−396.
(47) (a) Kober, E. M.; Caspar, J. V.; Lumpkin, R. S.; Meyer, T. J. *J. Phys. Chem.* **1983**, *87*, 952. (b) Meyer, T. J. *Acc. Chem. Res.* **1989**, *22*, 163.
(48) (a) Dietrich-Buchecker, C. O.; Marnot, P. A.; Sauvage, J.-P.; Kirchoff, J. R.; McMillin, D. R. *J. Chem. Soc., Chem. Commun.* **1983**, 513. (b) Ruthkosky, M.; Castellano, F. N.; Meyer, G. J. *Inorg. Chem.* **1996**, *35*, 6406. (c) Miller, M. T.; Gantzel, P. K.; Karpishin, T. B. *Inorg. Chem.* **1999**, *38*, 3414. (d) Riesgo, E. C.; Hu, Y.-Z.; Bouvier, F.; Thummel, R. P.; Scaltrito, D. V.; Meyer, G. J. *Inorg. Chem.* **2001**, *40*, 3413.
(49) Berger, R. M.; McMillin, D. R.; Dallinger, R. F. *Inorg. Chem.* **1987**, *26*, 3803.
(50) A reviewer suggested an alternative model wherein an equilibrium exists between an emissive four-coordinate compound and a nonemissive or near-IR emissive shorter-lived five-coordinate compound. For this model to be consistent with our observations, the photoluminesce and absorption data must report on the four-coordinate excited state and the X-rays probe the five-coordinate state.

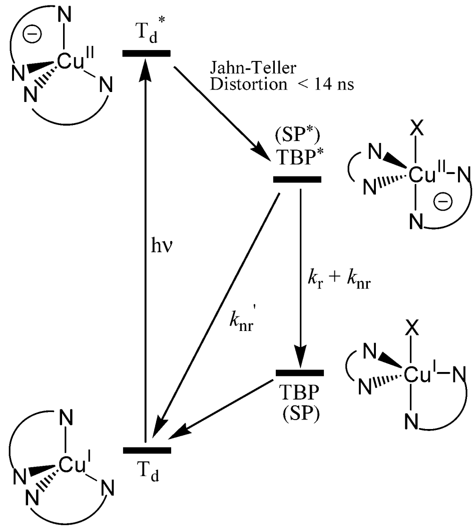

Figure 6. Four-state model consistent with X-ray, UV−vis, and photoluminescent studies of $[Cu^I(dmp)_2^+](BArF)$ in toluene. Light excitation of the ground-state $Cu^I(dmp)_2^+$, T_d, produces a Franck−Condon state, T_d*, with the same geometry. Within the time resolution of the experiment, this state relaxes to a distorted trigonal bipyramidal, TBP*, or square-pyramidal, SP* geometry with addition of an exogenous ligand, X, presumed to be derived from toluene or the BArF anion. Concerted nonradiative decay, k_{nr}', to the T_d ground state as well as radiative, k_r, and nonradiative decay, k_{nr}, yields a five-coordinate TBP or SP Cu^I geometry.

Radiative decay is a vertical process where the product must maintain the same nuclear coordinates and geometry as the excited state. Nonradiative decay, on the other hand, can lead directly to ground-state products. Therefore, light absorption and light emission involve different states with unique geometries that are not simply vibrational excited states of each other, as is often the case. This requires a minimum of four states, as shown schematically. Furthermore, radiative decay must yield a five-coordinate Cu(I) compound that subsequently releases the fifth ligand and distorts to yield the pseudo-tetrahedral ground state. This model shares many similarities with the "square schemes" used to rationalize thermal $Cu^{II/I}$ electron transfer in biomimetic model compounds which support the entactic state hypothesis.[21,22]

Conclusions

Structural information about molecular excited states by X-rays has been realized for the first time in solution on a nanosecond time scale. The experiments were performed in fluid solution at room temperature and thus under conditions meaningful for many applications of luminescent excited states. Our data support previous studies that have inferred large structural changes in copper diimine excited states. They have also revealed previously unrecognized behavior on the dynamics of excited-state structural reorganization. With a 14 ns time resolution, the X-ray probe pulse cluster captured the molecular structure of a thermally equilibrated MLCT state generated by laser illumination. Light excitation initiates complete charge transfer from copper to a dmp ligand and an inner-sphere reorganization that changed the coordination number from four to five and the geometry from tetrahedral to a likely distorted trigonal bipyramidal. An increase in the Cu−ligand bond distances was also observed. Since the excited state probed by X-rays is photoluminescent,[50] in accordance with the Franck−Condon principle, the product of radiative recombination must yield a five-coordinate Cu(I) compound that is not simply a vibrationally excited ground state. Therefore, light absorption and emission involve two distinct geometries, and at least four states are involved in the photophysics. These studies provide important new details and direct structural information on the inner-sphere reorganization that is novel to $Cu^{II/I}$ electron transfer. More generally, this study demonstrates that time domain XANES and XAFS can be used to quantify transient light-driven charge-transfer excited-state structural reorganization on short time scales.

Acknowledgment. This work is supported by the Division of Chemical Sciences, Office of Basic Energy Sciences, U.S. Department of Energy, under Contract W-31-109-Eng-38, and by the donors of the Petroleum Research Fund. The authors thank Drs. Wighard Jäger, Anneli Munkholm, Mark Beno, Jennifer Linton, and staff members at BESSRC-CAT, Advanced Photon Source, for their technical assistance.

JA017214G